Aerosol and Air Quality Research, 19: 92–102, 2019

ISSN: 1680-8584 print / 2071-1409 online
doi: 10.4209/aaqr.2017.12.0559

Source Apportionment of Rare Earth Elements in $PM_{2.5}$ in a Southeast Coastal City of China

Gongren Hu[1], Shanshan Wang[1], Ruilian Yu[1*], Zongwei Zhang[1], Xiaoming Wang[2]

[1] *College of Chemical Engineering, Huaqiao University, Xiamen 361021, China*
[2] *Analytical Laboratory of Beijing Research Institute of Uranium Geology, Beijing 100029, China*

ABSTRACT

In order to study the geochemical characteristics and sources of rare earth elements (REEs) in the $PM_{2.5}$ in Quanzhou City, 116 $PM_{2.5}$ samples were collected from three functional areas in the city during each season. The REE compositions and distribution patterns were then analyzed, together with ternary diagrams, to investigate the main provenance of these elements. Additionally, the sources of $PM_{2.5}$ were traced using a diagram of the Nd isotope ratio versus REE characteristics. The concentrations of the total rare earth elements (ΣREE), total light rare earth elements (ΣLREE) and total heavy rare earth elements (ΣHREE) in the $PM_{2.5}$ vary across both the four seasons (summer > spring > winter > autumn) and different functional areas (residential and industrial area > residential and commercial area > scenic area). There are significant correlations between ΣREE in the $PM_{2.5}$ and the $PM_{2.5}$ mass concentration in spring, summer and winter but none in autumn. The chondrite-normalized REE patterns in the $PM_{2.5}$ and potential-source samples are all rightward inclined, with the enrichment of LREE relative to HREE, and display obvious negative Eu anomalies. Results of the La-Ce-Sm diagram demonstrate that the REEs in the $PM_{2.5}$ of all functional areas are mainly derived from sources other than soil dust. The sources of REEs in the $PM_{2.5}$ across the four seasons and the reasons for spatial differences in the REEs across various functional areas can be determined via the La-Ce-V ternary diagram. The diagram of $^{143}Nd/^{144}Nd$ versus LREE/HREE suggests that the levels of REEs in the $PM_{2.5}$ in Quanzhou City are mainly affected by vehicle exhaust, followed by coal combustion and construction dust, and less influenced by soil dust and steelworks emissions.

Keywords: $PM_{2.5}$; Rare earth elements; Nd isotope; Geochemical characteristics; Source analysis.

INTRODUCTION

Fine particulate matter (particulate with the aerodynamic diameter no larger than 2.5 μm, designated as $PM_{2.5}$) has drawn worldwide attention for its adverse impact on air quality and human health. A growing number of evidence from epidemiologic studies has indicated that there is a strong link between elevated ambient concentrations of $PM_{2.5}$ and increased mortality and morbidity (Schwartz *et al.*, 1996; Peters *et al.*, 1997; Chen *et al.*, 2008; Chen *et al.*, 2013).

Many elements in $PM_{2.5}$, including toxic elements, such as As, Cd, Cr, Pb and Hg, have been reported (Pastuszka *et al.*, 2010; Tan *et al.*, 2014; Zhai *et al.*, 2014). In addition, platinum-group elements (PGEs), such as Pt, Pd and Rh, were also focused in $PM_{2.5}$ on concerning anthropogenic emission from automobiles (Bozlaker *et al.*, 2014). However, reports on rare- earth elements (REEs) in $PM_{2.5}$ are relatively few. REEs are usually divided into light rare earth elements (LREEs, including La, Ce, Pr, Nd, Pm, Sm and Eu) and heavy rare earth elements (HREEs, including Gd, Tb, Dy, Ho, Er, Tm, Yb, Lu, Y and Sc). REEs are widely used for industrial and medical materials, such as ceramics as superconductors, catalysts for automobiles (Ce), lasers (Nd), permanent magnets (Sm, Nd), fluorescent for color TVs (Eu, Y), fluorescent lamps (Eu), contrast medium for MRI (Gd), and so on, thus it can be considered that large amounts of REEs have been consumed and emitted into environment including the atmosphere (Krachler *et al.*, 2003). Although the concentrations of REEs in $PM_{2.5}$ are relatively low, they may pose a potential threat to human health (Zhang *et al.*, 2000).

REEs have similar chemical properties and they are generally considered to be resistant to fractionation in supracrustal environments (Nesbitt, 1979). The composition and distribution pattern of REEs are hardly influenced by the processes of weathering, transportation, sedimentation and diagenesis, hence the provenance information carried by REEs remains essentially unchanged, consequently REEs have been widely used to trace the provenance of

* Corresponding author.
Tel.: +86-592-6162300
E-mail address: ruiliany@hqu.edu.cn

sediment (Mclennan, 1989; Nesbitt *et al.*, 1990; Murray *et al.*, 1991; Jiang *et al.*, 2009; Xu *et al.*, 2012; Zhang *et al.*, 2018) and atmospheric particulates (Yang *et al.*, 2007; Moreno *et al.*, 2008; Bozlaker *et al.*, 2013; Zhao *et al.*, 2017). The characteristic parameters of REEs are strongly related to the constituent sources.

Similar to Pb and Sr isotopes, Nd isotope composition can also be used as an effective environmental indicator (Liu *et al.*, 1994; Nakano *et al.*, 2004; Geagea *et al.*, 2007; Geagea *et al.*, 2008; Awasthi *et al.*, 2018). It was reported that Nd isotope composition such as $^{143}Nd/^{144}Nd$ of desert dust and blown dust substance presented tiny fractionation during the weathering, transportation and sedimentation process (Chen *et al.*, 2007; Rao *et al.*, 2008).

In this study, 116 $PM_{2.5}$ samples were collected from different functional areas of Quanzhou City in four seasons, then the compositions and distribution patterns of REEs were analyzed, combined with La-Ce-Sm and La-Ce-V ternary diagrams to investigate the main provenance of REEs in $PM_{2.5}$. $PM_{2.5}$ sources in Quanzhou City were traced as well through the combination of Nd isotope with REE characteristic parameters in $PM_{2.5}$ samples and potential-source samples.

METHODS

Study Area

Quanzhou City (24°22′–25°56′N, 117°34′–119°05′E), with the total area of 11,015 km^2, is located in the southeast coast of Fujian Province, China. There is a typical subtropical maritime monsoon climate, and the weather is warm and humid with long-time sunshine and abundant rainfall. The mean annual temperature is 21°C. The prevailing wind direction is south wind from April to September, while northeast wind from October to March. As one of the economic development zones on the west side of Taiwan Strait, Quanzhou City has got a rapid increase in population, transportation, industrial and agricultural development over the past few decades, followed by an increasing pressure of air pollution. Petrochemical, electronic information and tourism services are the three major emerging industries in this city. By the end of 2016, the total population is about 8.5 million, and the number of motor vehicles is more than 2.2 million in Quanzhou City.

Sampling

Five sampling sites, located in Qingyuan Mountain Scenic Area (BG), residential and commercial area (RD1–RD2), residential and industrial area (ID), were set according to the distribution of different functional areas in Quanzhou City. The specific information about the sampling sites is shown in Table 1, and the distribution of sampling sites is presented in Fig. 1.

$PM_{2.5}$ samples were synchronously collected at each sampling site in four seasons. The specific sampling periods for spring, summer, autumn and winter are as follows: March 30, 2014, to April 1, 2014; July 17, 2014, to July 27, 2014; October 1, 2014, to October 7, 2014; January 8, 2015, to January 14, 2015. Meteorological conditions like barometric pressure, average temperature, and weather were recorded during the sampling period. Every sample was taken for 23 h continuously (8:00 a.m. to 7:00 a.m. in the next day), and total 116 $PM_{2.5}$ samples were collected (four samples were missed due to the fault of sampling apparatus).

TH-150C III samplers (Wuhan Tianhong Ltd., China) were employed to collect $PM_{2.5}$ samples. Before sampling, the $PM_{2.5}$ cutters were cleaned and the samplers were calibrated with a sampling flow rate of 100 L min^{-1}. Polypropylene filters were used for $PM_{2.5}$ sampling. Before and after sampling, the filters were kept in a clean environment with constant temperature (20 ± 1°C) and humidity (50 ± 2%) for 24 hours to get the constant weights. A electronic analysis balance (Sartorius t-114) was used to

Table 1. Specific description of $PM_{2.5}$ sampling sites.

Site	Functional area	Longitude	Latitude	Height (m)	Detail description
BG	Scenic area	118°35′E	24°56′N	7	Located in a private house roof in Qingyuan. Street ring village, an urban-rural fringe. There is no construction around 200 m sphere.
RD1	Residential and commercial area	118°35′E	24°54′N	9	Located in the building roof of Bank of China, Jiuyi Street in Licheng District, central urban area. There are some construction sites within the perimeter of 200 m.
RD2	Residential and commercial area	118°36′E	24°54′N	24	Located in a residential building roof of New Fengze village in Fengze District, center of the city. There are some construction sites within the perimeter of 200 m.
RD3	Residential and commercial area	118°39′E	24°55′N	10	Located in a private house roof in Dongfu Road, Chengdong Street in Fengze District, suburb. There are some construction sites around 200 m.
ID	Residential and industrial area	118°33′E	24°52′N	12	Located in an office building roof in Qingmeng. Industrial Park, the Economic and Technological. Development Zone of Quanzhou city. There are several construction sites within 200 m.

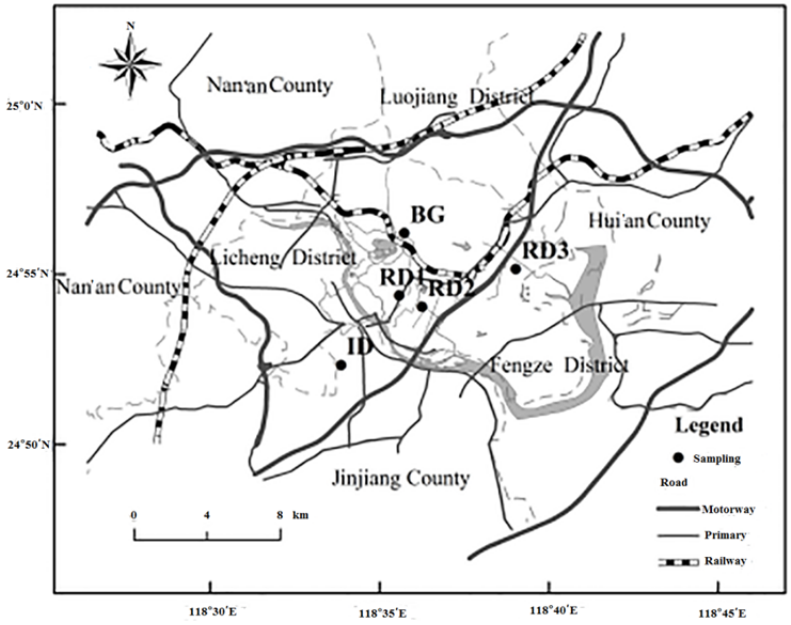

Fig. 1. Map of sampling sites of atmospheric $PM_{2.5}$ in Quanzhou City.

weigh the quality of filter membrane, the accuracy was 0.01 mg. The net weight of a $PM_{2.5}$ sample was calculated by the mass difference of the filter before and after sampling.

Based on the detailed investigation of traffic, industry and construction distribution in Quanzhou City, combined with industrial layout, energy consumption and other potential pollution sources, five potential sources of $PM_{2.5}$ including the vehicle emission, coal-fired power plant dust, cement plant dust, steelworks emission and soil dust, were collected during the $PM_{2.5}$ sampling period. Two sampling sites were set for each potential source. The vehicle emission dusts were collected with a brush at the traffic roadsides of Pingshan tunnel and Donghai tunnel. The potential source samples of coal-fired power plant dust, cement plant fly ash, iron and steel plant sintered fly ash were collected from Shishi coal-fired power plant, Anxi Hutou cement plant and the steel plant, respectively. Two soil dust samples were collected as natural sources according to the distribution of soil types within the urban built area and surrounding 10 km.

Determination of REEs and Quality Assurance

A quarter of each $PM_{2.5}$ sampling filter was cut into pieces and put into a tetrafluoroethylene crucible, then 0.8 mL HNO_3 and 1–2 drops HF were added. The mixture was heated in a 130°C dryer for 5 h. Then, the cap was unscrewed to remove volatile organic compounds (VOCs) and the mixture was heated in a 180°C dryer for 12 h again. Then, the mixture was heated on an electro-thermal board till dryness. Then, 0.5 mL HNO_3 was added, and the mixture was heated again continuously to completely dry. Then, 0.2 mL (50 μg mL^{-1}) Rh as internal standard solution, 0.3 mL HNO_3 and 0.1 mL ultrapure water were added into the tetrafluoroethylene crucible and heated in a 140°C dryer for another 5 h. After cooled, the solution was diluted with ultrapure water to 2 mL for further analysis.

For every 10 $PM_{2.5}$ samples, one sample was randomly selected for triplicate experiments. A blank filter was processed using the same digestion procedure for each batch of samples. Each potential-source sample was digested according to the procedure described by Zhao *et al.* (2017).

Concentrations of REEs in the digestion solutions were determined by inductively coupled plasma mass spectrometry (ICP-MS, Elan DRC-e, PerkinElmer). Blanks were subtracted from the samples. A soil reference material (GSS-7) was used to ensure the accuracy and precision of the analysis method. The detection limits for REEs were 0.002 μg g^{-1} to 0.006 μg g^{-1}. The relative standard deviation was less than 5.0%. And the recoveries were within 91.3% to 106.7%.

Determination of Nd Isotope Ratio and Quality Assurance

The separation and purification for Nd isotope was processed according to the national analytical procedure of GB/T 17672-1999. The ratio of $^{143}Nd/^{144}Nd$ was determined using VG354 thermal ionization mass spectrometry (TI-MS). A solution of Nd isotope reference material (JMC) was employed to check the reproducibility and accuracy of the analysis of Nd isotope ratio, and the measured $^{143}Nd/^{144}Nd$ of JMC was 0.511986 ± 0.000022.

RESULTS AND DISCUSSION

Characteristics of REE Concentrations in $PM_{2.5}$

The mean concentrations of total rare earth elements (ΣREE), light rare earth elements (ΣLREE) and heavy rare earth elements (ΣHREE) in atmospheric $PM_{2.5}$ in Quanzhou City are shown in Fig. 2(a). The mean values of ΣREE, ΣLREE and ΣHREE are 3.32 ng m^{-3}, 3.03 ng m^{-3} and 0.29 ng m^{-3}, respectively. Light rare earths account for 91% of the total rare earth content, which is similar to the distribution characteristics of rare earth elements in atmospheric particulates in some cities (Tang *et al.*, 2013),

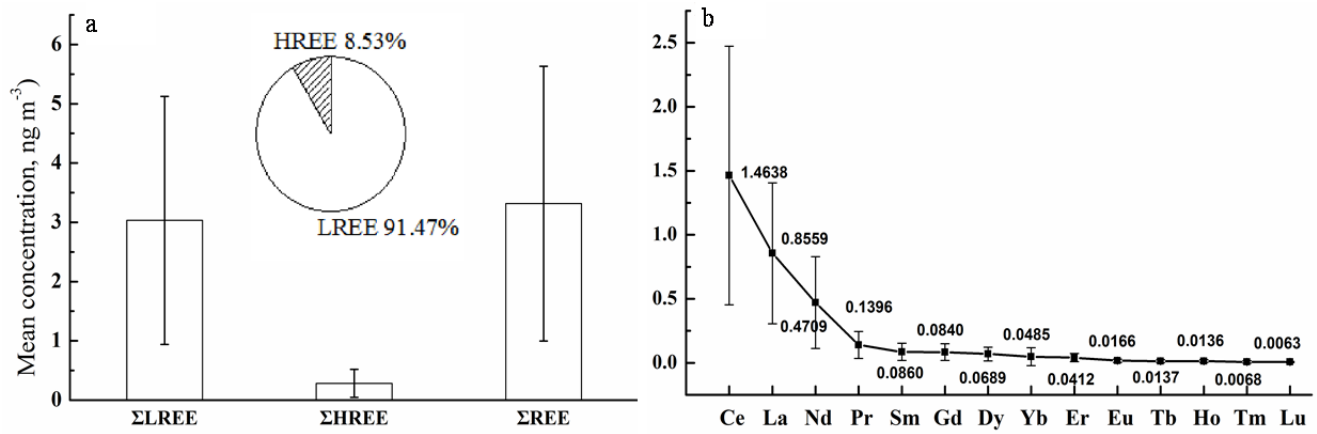

Fig. 2. (a) Mean concentrations of ΣREE, ΣLREE and ΣHREE in atmospheric $PM_{2.5}$ and (b) Mean concentrations of rare earth elements in atmospheric $PM_{2.5}$.

manifesting that atmospheric particulates in these cities are characterized by enrichment of light rare earth elements.

As demonstrated in Fig. 2(b), the mean concentrations of 14 rare earth elements (arranged in a descending order, including standard deviation) in $PM_{2.5}$ in Quanzhou City show the sequence of Ce > La > Nd > Pr > Sm > Gd > Dy > Yb > Er > Eu > Tb > Ho > Tm > Lu, basically consistent with the abundance rank of rare earth elements in the upper crust, indicating that the distribution of rare earth elements in $PM_{2.5}$ in Quanzhou City is controlled by the crustal abundance of elements.

Seasonal Variation of REE Concentrations

The distributions of $PM_{2.5}$, ΣLREE, ΣHREE and ΣREE in $PM_{2.5}$ in Quanzhou City in different seasons are listed in Table 2. ΣLREE, ΣHREE and ΣREE in $PM_{2.5}$ in summer are obviously higher than those in other seasons, which might be related to the higher wind speed during the summer sampling period. The higher wind speed can increase the ground floating dust, and then increase the proportion of dust in $PM_{2.5}$, resulting in the rise of the contents of rare earth elements in $PM_{2.5}$.

As shown in Table 2, the minimum values of $PM_{2.5}$, ΣREE, ΣLREE and ΣHREE appear in winter samples. According to the observation of all samples in winter, the minimum value of ΣREE in each functional area appears in the $PM_{2.5}$ samples collected on January 13, 2015. Combining with the seasonal distribution of $PM_{2.5}$ mass concentration, it is discovered that other sampling sites, except sites BG and RD1, also show an extremely low concentration of $PM_{2.5}$ on this day. Meanwhile, the seasonal distribution of ΣREE in $PM_{2.5}$ is similar to the seasonal distribution of $PM_{2.5}$ mass concentration (spring, summer > autumn, winter), which suggests that the REE concentration in $PM_{2.5}$ is correlated to the concentration of $PM_{2.5}$ to some extent.

The mean concentrations of 14 rare earth elements (arranged in a descending order, including standard deviation) in $PM_{2.5}$ in different seasons of Quanzhou City are shown in Fig. 3. It is found that the mean concentration sequences of REEs in $PM_{2.5}$ in various seasons basically meet the even number rule (Oddo–Harkins law). The standard deviation values of La, Ce and Nd in $PM_{2.5}$ in four seasons are relatively large, which reflects the concentration instability of these elements, i.e., other sources besides soil dust might also have an influence on the REE concentration.

Distribution Characteristics of REEs in Different Functional Areas

Distribution characteristics of ΣLREE, ΣHREE and ΣREE in $PM_{2.5}$ in different functional areas are listed in Table 3. The values of ΣLREE, ΣHREE and ΣREE are obviously different in different functional areas with the order of residential and industrial area > residential and commercial area > scenic area, which is consistent with the distribution of $PM_{2.5}$ mass concentration in different functional areas. As shown in Fig. 4, the mean concentrations of REEs (arranged in a descending order, including standard deviation) in $PM_{2.5}$ in different functional areas of Quanzhou City also basically meet the Oddo–Harkins law. The standard deviation values of La, Ce and Nd in residential and industrial area are greater than those in other functional areas, implying the instability of sources.

Correlation between ΣREE and $PM_{2.5}$ Concentrations in Different Seasons

Linear regression fitting was conducted for $PM_{2.5}$ mass concentration and ΣREE in $PM_{2.5}$ samples in the four seasons of Quanzhou City, as shown in Fig. 5. The results demonstrate that there is a significant correlation between ΣREE in $PM_{2.5}$ and $PM_{2.5}$ mass concentration in spring, summer and winter. Nevertheless, there is no correlation between ΣREE in $PM_{2.5}$ and $PM_{2.5}$ mass concentration in autumn. Hence, the ΣREE in $PM_{2.5}$ is not only associated with $PM_{2.5}$ mass concentration, but also influenced by other factors in autumn, such as the difference of dilution intensity caused by gale weather or injection of exogenous rare earths.

Distribution Patterns of REEs in $PM_{2.5}$ in Different Seasons

In order to comprehend whether REEs in $PM_{2.5}$ undergo exogenous influences, REEs in $PM_{2.5}$ and potential-source

Table 2. Seasonal distribution of ΣLREE, ΣHREE and ΣREE in $PM_{2.5}$.

	$PM_{2.5}$ (μg m^{-3})	ΣLREE (ng m^{-3})	ΣHREE (ng m^{-3})	ΣREE (ng m^{-3})
Spring (n = 15)	60.00 (35.21–103.37)	2.93 (1.04–7.82)	0.21 (0.05–0.70)	3.14 (1.09–8.51)
Summer (n = 34)	41.41 (16.00–83.50)	4.82 (1.65–10.28)	0.48 (0.09–1.43)	5.29 (1.74–11.70)
Autumn (n = 34)	30.26 (15.89–54.52)	2.36 (0.56–6.78)	0.22 (0.04–0.75)	2.58 (0.60–7.53)
Winter (n = 33)	30.53 (7.19–60.38)	2.46 (0.12–11.17)	0.24 (0.01–1.15)	2.70 (0.13–12.32)

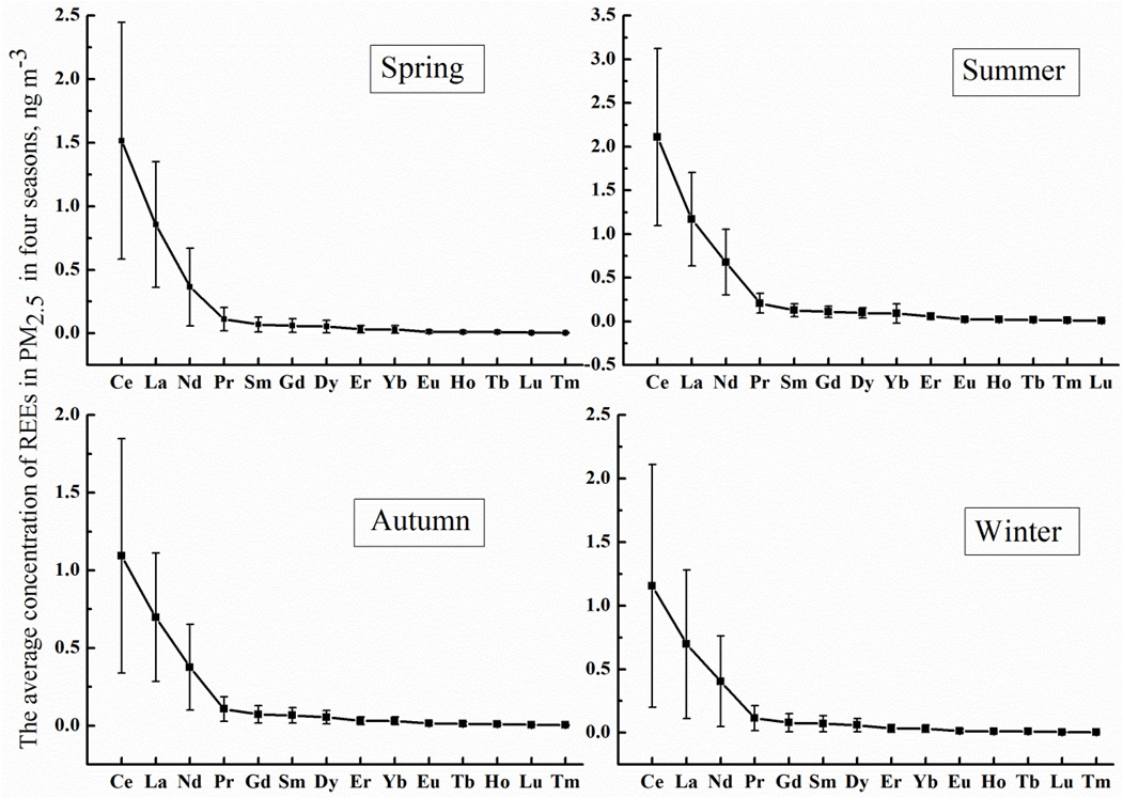

Fig. 3. Mean concentrations of REEs in $PM_{2.5}$ in four seasons.

Table 3. Summary of ΣLREE, ΣHREE and ΣREE in $PM_{2.5}$ in different functional areas (ng m^{-3}).

	ΣLREE	ΣHREE	ΣREE
Scenic area (n = 24)	1.79 (0.12–4.48)	0.15 (0.01–0.42)	1.94 (0.13–4.91)
Residential and commercial area (n = 70)	3.29 (0.13–8.10)	0.30 (0.02–0.75)	3.59 (0.15–8.79)
Residential and industrial area (n = 22)	3.59 (0.36–11.17)	0.38 (0.04–1.43)	3.96 (0.40–12.32)

samples collected from different functional areas in Quanzhou City in four seasons were normalized using the average REE values of 6 Leedy chondrites. As shown in Fig. 6, 6(a), 6(b), 6(c), and 6(d) are the distribution patterns of REEs in spring, summer, autumn and winter, respectively. The geometric shape of REE distribution pattern has a significant denotative meaning. On the whole, all the REE distribution patterns lean rightward with the La-Eu part relatively steep while the Gd-Lu part comparatively gentle. For all the REE distribution patterns, LREEs show more enrichment than HREEs, and obvious Eu negative anomaly exists. In spring, the shapes of La-Er in $PM_{2.5}$ samples from all functional areas are similar with those of all investigated potential sources, but the shapes of Tm-Lu in $PM_{2.5}$ samples from all functional areas (especially residential and industrial area) are obviously different with those of all investigated potential sources, demonstrating that not only all the investigated potential sources but also other uninvestigated sources have an impact on the REEs in $PM_{2.5}$. In summer, the REE curve of $PM_{2.5}$ in scenic area is similar with those of all investigated potential sources, suggesting that the REEs in $PM_{2.5}$ of scenic area mainly derive from all investigated potential sources. The shapes of La-Er in $PM_{2.5}$ samples from the other functional areas are similar with those of all investigated potential sources, but the shapes of Tm-Lu in $PM_{2.5}$ samples are different with those of all investigated potential sources, demonstrating that not only all the investigated potential sources but also other uninvestigated sources have an impact on the REEs in $PM_{2.5}$ in the other functional areas in summer. In autumn,

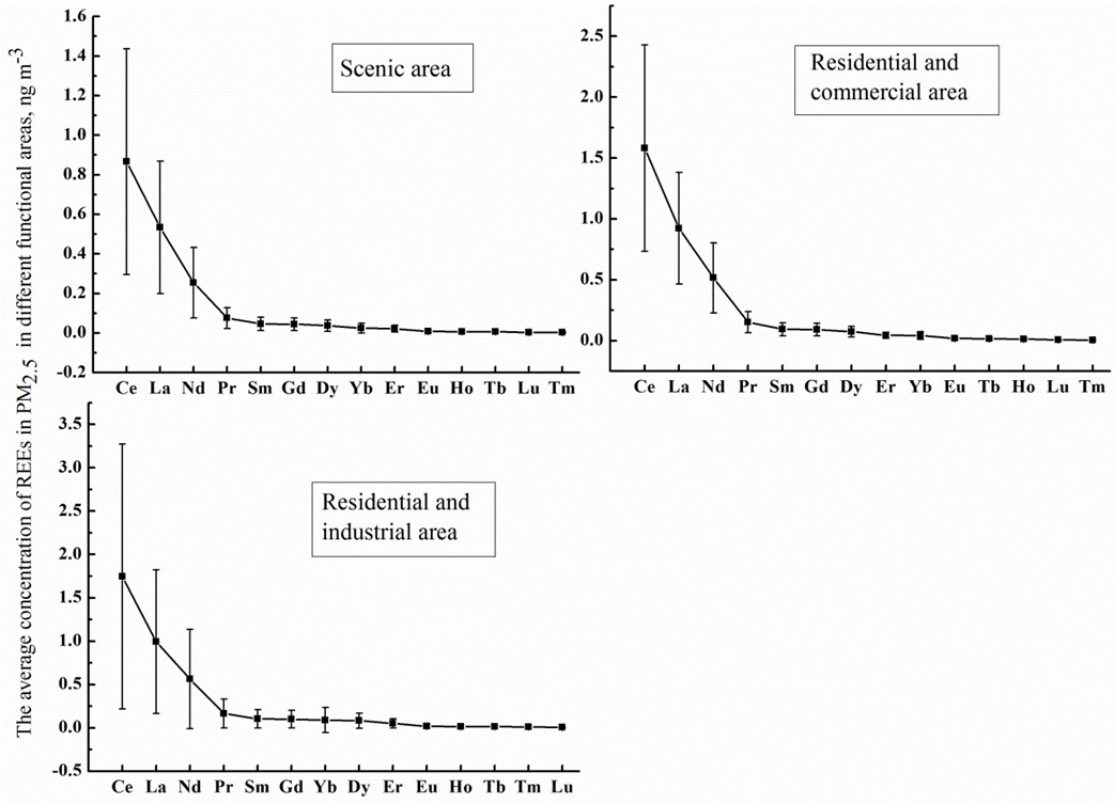

Fig. 4. Mean concentrations of REEs in $PM_{2.5}$ in different functional areas.

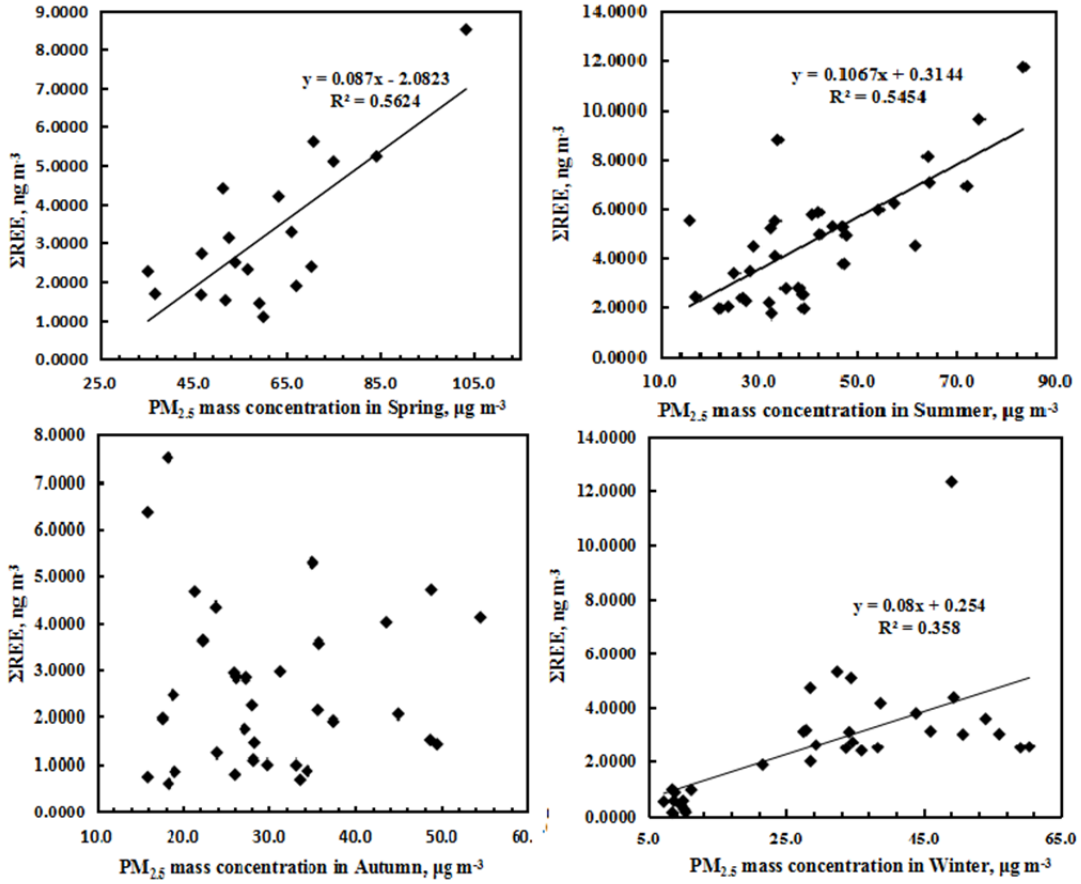

Fig. 5. Correlation between ΣREE and $PM_{2.5}$ concentration in different seasons.

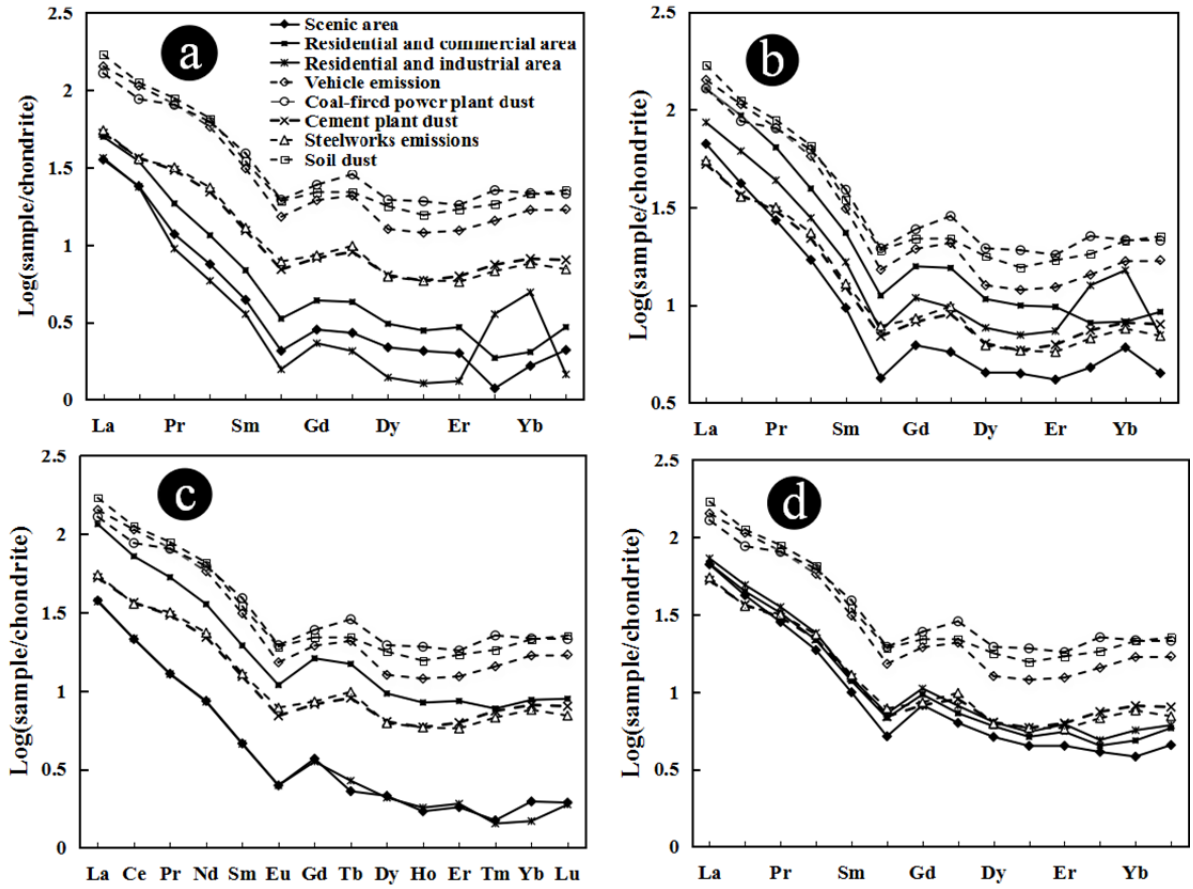

Fig. 6. Chondrite-normalized REE patterns in $PM_{2.5}$ samples and potential sources in different functional areas in four seasons (a: spring, b: summer, c: autumn, and d: winter).

the shapes of La-Gd in $PM_{2.5}$ samples from all functional areas are similar with those of all investigated potential sources, but the shapes of Tb-Lu in $PM_{2.5}$ samples from all functional areas are different with those of all investigated potential sources, implying that not only all the investigated potential sources but also other uninvestigated sources have an impact on the REEs in $PM_{2.5}$ from all functional areas in autumn. It is worth noting that the REE curve of $PM_{2.5}$ in residential and industrial area almost overlaps with that in scenic area in autumn, indicating that the sources of REEs in $PM_{2.5}$ from these two functional areas are almost the same in autumn. The REE curves of $PM_{2.5}$ in residential and commercial area and residential and industrial area in summer and the REE curves of $PM_{2.5}$ in residential and commercial area in autumn are between the REE curves of all five investigated potential sources, implying that the REEs in $PM_{2.5}$ might come from the highly mixed substances in different source regions in the process of wind-force transportation in summer and autumn. In winter, the REE curves in $PM_{2.5}$ from three functional areas are very similar and close to each other, and are all close to those of cement plant dust and steelworks emissions, demonstrating that the above two sources might have a significant influence on the REEs in $PM_{2.5}$ from all functional areas in winter. The REE distribution curves of $PM_{2.5}$ samples from residential and industrial area in spring and summer show a great difference from those of other $PM_{2.5}$ samples and the investigated potential sources in the aspect of HREE. Such difference might be caused by the fact that a special pollution source entered the atmospheric environment during the sampling period. It should be also noticed that the REE distribution patterns of the five investigated potential-source samples do not present an obvious difference, i.e., the specific sources of REEs in $PM_{2.5}$ samples in various functional areas cannot be clearly judged only through the REE distribution patterns.

Qualitative Identification on Sources of LREEs in $PM_{2.5}$ in Different Seasons Using Ternary Diagrams

La-Ce-Sm Ternary Diagram

The degree of exogenous influence on REEs in $PM_{2.5}$ can be judged using La-Ce-Sm ternary diagram, in which La and Sm are usually multiplied by 2 and 10 respectively since the abundance of Ce is about 2 and 10 times of those of La and Sm, respectively (Moreno *et al.*, 2008). In Figs. 7(a), 7(b), 7(c), and, 7(d) are the ternary diagrams of La-Ce-Sm in $PM_{2.5}$ in spring, summer, autumn and winter in Quanzhou City. Commonly, contamination-free REEs from the earth crust will be distributed in the central position of La-Ce-Sm ternary diagram. In this study, soil dust samples collected in Quanzhou City are almost distributed in the center of La-Ce-Sm ternary diagram. All

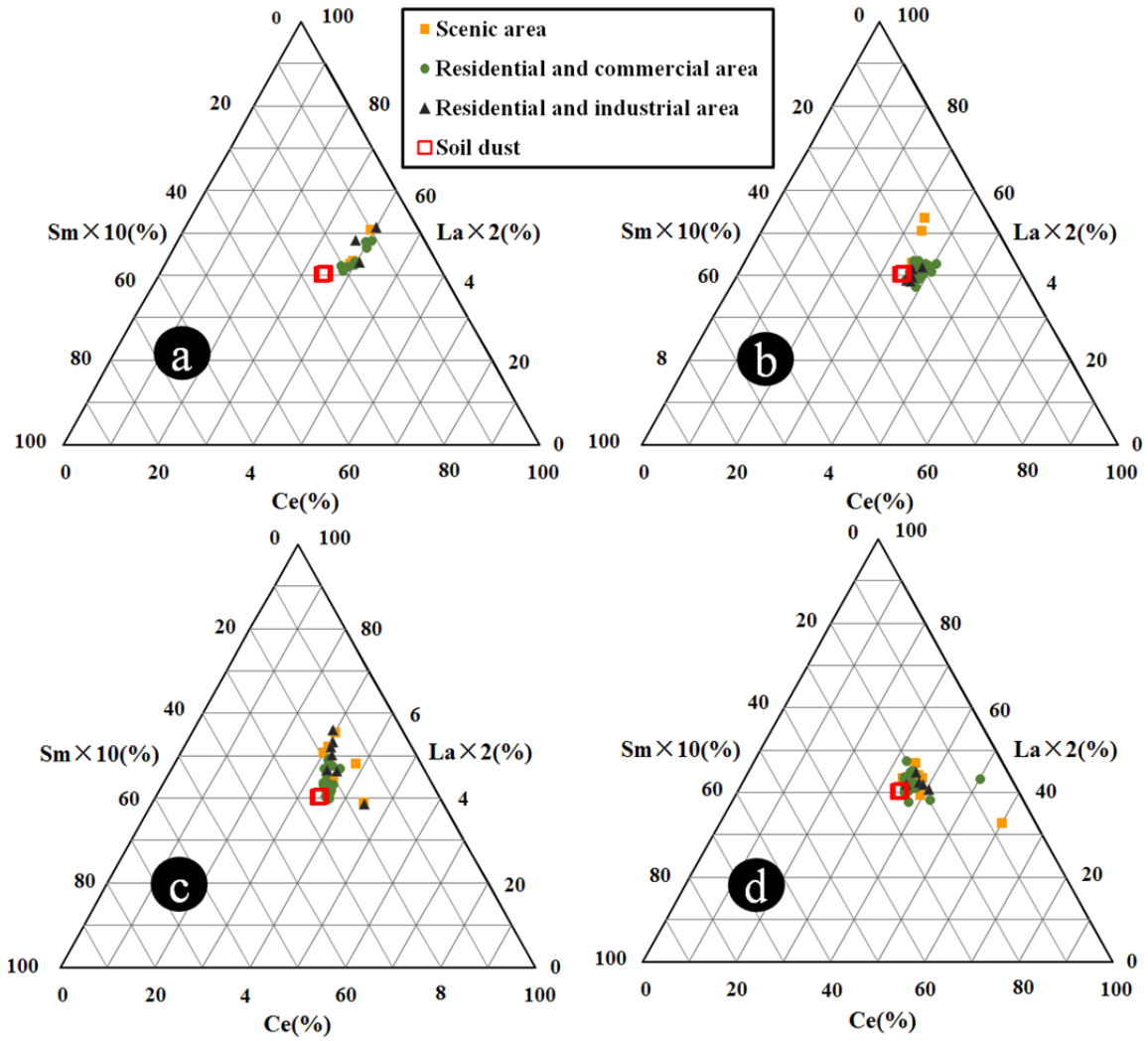

Fig. 7. La-Ce-Sm ternary diagrams in $PM_{2.5}$ of different functional areas in four seasons (a: spring, b: summer, c: autumn, and d: winter).

$PM_{2.5}$ samples collected in spring are beyond the scope of soil dust, which means that soil dust is not the main source of REEs in $PM_{2.5}$ in spring. Additionally, the scatters of $PM_{2.5}$ samples in the other seasons partially superpose soil dust samples, but are roughly distributed to the upper right of soil dust, manifesting that the REEs in $PM_{2.5}$ in Quanzhou City is influenced by other sources besides soil dust. Except several special samples, the relative percentage change scopes of La, Ce and Sm in most $PM_{2.5}$ samples are insignificant, and no obvious difference is observed among $PM_{2.5}$ samples in three functional areas.

La-Ce-V Ternary Diagram

La-Ce-V ternary diagram was introduced for further analysis, so as to confirm the sources of $PM_{2.5}$ in different seasons in Quanzhou City, and to discuss the reasons for the spatial difference of REEs in various functional areas. La-Ce-V ternary diagrams of $PM_{2.5}$ and potential-source samples in spring, summer, autumn and winter in Quanzhou City are shown in (a), (b), (c) and (d) in Fig. 8, respectively.

In spring, the percentage scopes of La, Ce and V in $PM_{2.5}$ samples are 0.6%–4%, 0.9%–7%, and 88%–98%, respectively, approaching cement plant dust samples, implying a direct influence by the construction dust.

In summer, $PM_{2.5}$ samples from residential and commercial area are in the linearity region formed by five potential sources, suggesting that the five investigated potential sources all contribute a part. The $PM_{2.5}$ samples of scenic area are more easily influenced by steelworks emissions, coal-fired power plant dust and construction dust. The $PM_{2.5}$ samples of residential and industrial area are mainly under the influence of coal combustion, steelworks emissions, soil dust and vehicle emission.

In autumn and winter, the $PM_{2.5}$ samples from scenic area are close to the scope of cement plant dust, so these $PM_{2.5}$ samples are directly influenced by construction dust. In autumn, $PM_{2.5}$ samples from residential and commercial area and residential and industrial area are within the scope constituted by cement plant dust and steelworks emissions, implying direct impacts of above two potential sources. In winter, $PM_{2.5}$ samples from residential and commercial area and residential and industrial area are in the linearity

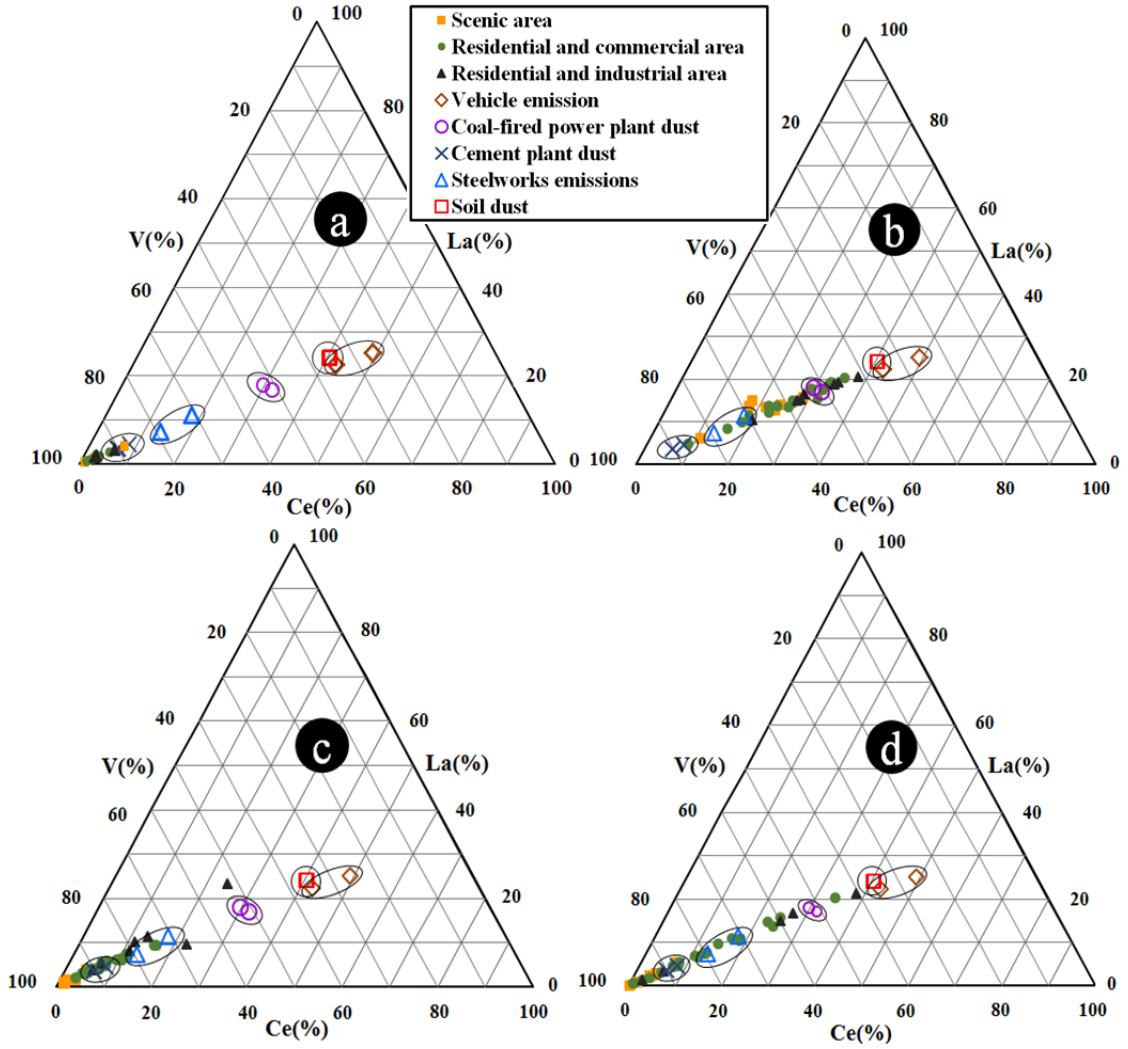

Fig. 8. Triangle diagram of La-Ce-V in $PM_{2.5}$ of different functional areas in four seasons and potential sources (a: spring, b: summer, c: autumn, and d: winter).

scope formed by five investigated potential sources, suggesting the joint influence by the five potential sources.

Tracing $PM_{2.5}$ Sources by Combining Nd Isotope with LREE/HREE

In order to explore the main sources of $PM_{2.5}$ in Quanzhou City, the diagram of $^{143}Nd/^{144}Nd$ versus LREE/HREE for some $PM_{2.5}$ and potential-source samples is plotted in Fig. 9. It is found that the scope of $PM_{2.5}$ samples are closer to the samples of vehicle emission, coal-fired power plant dust and cement plant dust, but a bit far from the samples of soil dust and steelworks emissions, implying that the REEs in $PM_{2.5}$ in Quanzhou City undergoes the largest influence from vehicle emission, followed by coal combustion and construction dust, while the influence of soil dust and steelworks emissions is relatively insignificant. REEs in $PM_{2.5}$ in another southeast Chinese city, Xiamen, were mainly originated from vehicle exhaust and not dominated by local natural soil (Wang *et al.*, 2017), which is similar to the conclusion of the present study. However, there are more industrial activities in Quanzhou City, causing REEs in $PM_{2.5}$ were influenced by other industrial sources such as coal combustion and cement plant in Quanzhou.

CONCLUSIONS

(1) ΣREE, ΣLREE and ΣHREE in the $PM_{2.5}$ in Quanzhou City range 0.13–12.32 ng m^{-3}, 0.12–11.17 ng m^{-3} and 0.01–1.43 ng m^{-3}, respectively. There are obvious differences in the ΣLREE, ΣHREE and ΣREE values among the $PM_{2.5}$ samples taken from different functional areas in different seasons. In terms of the area, the values for ΣREE, ΣLREE and ΣHREE exhibit the sequence: residential and industrial area > residential and commercial area > scenic area. In terms of the season, ΣREE, ΣLREE and ΣHREE are obviously higher during summer.

(2) There are significant correlations between ΣREE in the $PM_{2.5}$ and the $PM_{2.5}$ mass concentration in spring, summer and winter but none in autumn. All the chondrite-normalized REE patterns in the $PM_{2.5}$ samples and potential sources lean rightward with LREE enrichment

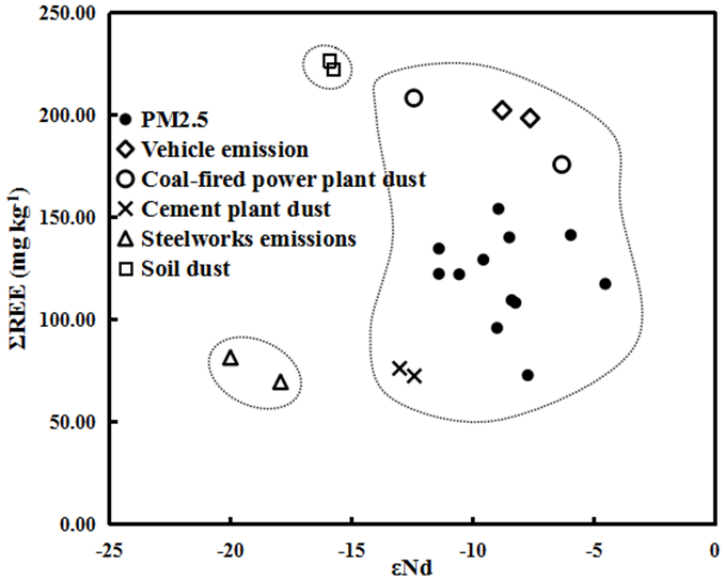

Fig. 9. Plot of $^{143}Nd/^{144}Nd$ versus LREE/HREE for some $PM_{2.5}$ and potential- source samples in Quanzhou City.

and an obvious Eu negative anomaly. There are no significant differences between the REE distribution curves for the investigated potential sources, i.e., specific sources of REEs in the $PM_{2.5}$ in various functional areas cannot be determined only by the REE distribution patterns.

(3) REEs in the $PM_{2.5}$ in Quanzhou City are influenced by sources other than soil dust, and soil dust is not a significant factor in spring, according to the LaCeSm ternary diagram. No obvious differences are exhibited by the $PM_{2.5}$ samples from the three functional areas. The sources of REEs in the $PM_{2.5}$ across the four seasons and the reasons for spatial differences in the REEs across various functional areas can be determined via the La-Ce-V ternary diagram.

(4) According to the diagram of $^{143}Nd/^{144}Nd$ versus LREE/HREE for some $PM_{2.5}$ and potential-source samples, the REEs in the $PM_{2.5}$ in Quanzhou City receive their largest contribution from traffic sources, followed by coal combustion and construction dust, while the influence of soil dust and steelworks emissions is insignificant.

ACKNOWLEDGMENTS

This work was supported by the National Natural Science Foundation of China (21477042, 21377042) and the Natural Science Foundation of Fujian Province (2016J01065). The authors thank to all the sampling staffs and colleagues who advise on this article.

REFERENCES

Awasthi, N., Ray, E. and Paul, D. (2018). Sr and Nd isotope compositions of alluvial sediments from the Ganga Basin and their use as potential proxies for source identification and apportionment. *Chem. Geol.* 476: 327–339.

Bozlaker, A., Buzcu-Guven, B., Fraser, M.P. and Chellam, S. (2013). Insights into PM_{10} sources in Houston, Texas: Role of petroleum refineries in enriching lanthanoid metals during episodic emission events. *Atmos. Environ.* 69: 109–117.

Bozlaker, A., Spada, N.J., Fraser, M.P. and Chellam, S. (2014). Elemental characterization of $PM_{2.5}$ and PM_{10} emitted from light duty vehicles in the Washburn Tunnel of Houston, Texas: Release of Rhodium, Palladium, and Platinum. *Environ. Sci. Technol.* 48: 54–62.

Chen, J., Li, G., Yang, J., Rao, W., Lu, H., Balsam, W., Sun, Y. and Ji, J. (2007). Nd and Sr isotopic characteristics of Chinese deserts: Implications for the provenances of Asian dust. *Geochim. Cosmochim. Acta* 71: 3904–3914.

Chen, J.M., Tan, M.G., Li, Y.L., Zheng, J., Zhang, Y.M., Shan, Z., Zhang, G.L. and Li, Y. (2008). Characteristics of trace elements and lead isotope ratios in $PM_{2.5}$ from four sites in Shanghai. *J. Hazard. Mater.* 156: 36–43.

Chen, R.J., Peng, R.D., Meng, X., Zhou, Z.J., Chen, B.H. and Kan, H.D. (2013). Seasonal variation in the acute effect of particulate air pollution on mortality in the China Air Pollution and Health Effects Study (CAPES). *Sci. Total Environ.* 450: 259–265.

Geagea, M.L., Stille, P., Millet, M. and Perrone, Th. (2007). REE characteristics and Pb, Sr and Nd isotopic compositions of steel plant emissions. *Sci. Total Environ.* 373: 404–419.

Geagea, M.L., Stille, P., Guathier-Lafaye, F. and Millet, M. (2008). Tracing of industrial aerosol sources in an urban environment using Pb, Sr, and Nd isotopes. *Environ. Sci. Technol.* 42: 692–698.

Jiang, F.Q., Zhou, X.J., Li, A.C. and Li, T.G. (2009). Quantitatively distinguishing sediments from the Yangtze River and the Yellow River using delta δEu-N-∑REEs pound plot. *Sci. China Ser. D* 52: 232–241.

Krachler, M., Mohl, C., Emons, H. and Shotyk, W. (2003).

Two thousand years of atmospheric rare earth element (REE) deposition as revealed by an ombrotrophic peat bog profile, Jura Mountains, Switzerland. *J. Environ. Monit.* 5: 111–121.

Liu, C.Q., Masuda, A., Okada, A., Yabuki, S. and Fan, Z.L. (1994). Isotope geochemistry of quaternary deposits from the arid lands in northern China. *Earth Planet. Sci. Lett.* 127: 25–38.

Mclennan, S.M. (1989). Rare earth elements and sedimentary rocks: Influence of provenance and sedimentary processes. *Rev. Mineral.* 2: 169–200.

Moreno, T., Querol, X., Alastuey, A. and Gibbons, W. (2008). Identification of FCC refinery atmospheric pollution events using lanthanoid- and vanadium-bearing aerosols. *Atmos. Environ.* 42: 7851–7861.

Murray, R.W., Brink, M.R.B., Brumsack, H.J., Gerlach, D. C. and Iii, G.P.R. (1991). Rare earth elements in Japan Sea sediments and diagenetic behavior of Ce/Ce*: Results from ODP Leg 127. *Geochim. Cosmochim. Acta* 55: 2453–2466.

Nakano, T. (2004). Regional Sr-Nd isotopic ratios of soil minerals in northern China as Asian dust fingerprints. *Atmos. Environ.* 38: 3061–3067.

Nesbitt, H.W. (1979). Mobility and fractionation of rare earth elements during weathering of a granodiorite. *Nature* 279: 206–210.

Nesbitt, H.W., Macrae, N.D. and Kronberg, B.I. (1990). Amazon deep-sea fan muds: Light REE enriched products of extreme chemical weathering. *Earth Planet. Sci. Lett.* 100: 118–123.

Pastuszka, J.S., Rogula-Kozlowska, W. and Zajusz-Zubek, E. (2010). Characterization of PM_{10} and $PM_{2.5}$ and associated heavy metals at the crossroads and urban background site in Zabrze, Upper Silesia, Poland, during the smog episodes. *Environ. Monit. Assess* 168: 613–627.

Peters, A., Wichmann, H.E., Tuch, T., Heinrich, J. and Heyder, J. (1997). Respiratory effects are associated with the number of ultrafine particles. *Am. J. Respir. Crit. Care Med.* 155: 1376–1383.

Rao, W., Chen, J., Yang, J., Ji, J., Li, G. and Tan, H. (2008). Sr-Nd isotopic characteristics of eolian deposits in the Erdos Desert and Chinese Loess Plateau: Implications for their provenances. *Geochem. J.* 42: 273–282.

Schwartz, J., Dockery, D.W. and Neas, L.M. (1996). Is daily mortality associated specifically with fine particles? *J. Air Waste Manage. Assoc.* 46: 927–939.

Tan, J.H., Duan, J.C., Ma, Y.L., Yang, F.M., Cheng, Y., He, K.B., Yu, Y.C. and Wang, J.W. (2014). Source of atmospheric heavy metals in winter in Foshan, China. *Sci. Total Environ.* 493: 262–270.

Tang, Y., Han, G.L., Wu, Q.X. and Xu, Z.F. (2013). Use of rare earth element patterns to trace the provenance of the atmospheric dust near Beijing, China. *Environ. Earth Sci.* 68: 871–879.

Wang, S., Yu, R., Hu, G., Hu, Q. and Zheng, Q. (2017). Distribution and source of rare earth elements in $PM_{2.5}$ in Xiamen, China. *Environ. Toxicol. Chem.* 36: 3217–3222.

Xu, F., Chen, S., Qiu, L. and Cao, Y. (2012). A preliminary reassessment of Eu_N-REEs plot for distinguishing sediment provenances. *J. Rare Earths* 30: 94–96.

Yang, X., Liu, Y., Li, C., Song, Y., Zhu, H. and Jin, X. (2007). Rare earth elements of aeolian deposits in Northern China and their implications for determining the provenance of dust storms in Beijing. *Geomorphology* 87: 365–377.

Zhai, Y.B., Liu, X.T., Chen, H.M., Xu, B.B., Zhu, L., Li, C.T. and Zeng, G.M. (2014). Source identification and potential ecological risk assessment of heavy metals in $PM_{2.5}$ from Changsha. *Sci. Total Environ.* 493: 109–115.

Zhang, H., Feng, J., Zhu, W.F., Liu, C.Q., Xu, S.Q., Shao, P.P., Wu, D.S., Yang, W.J. and Gu, J.H. (2000). Chronic toxicity of rare-earth elements on human beings - Implications of blood biochemical indices in REE-high regions, South Jiangxi. *Biol. Trace Elem. Res.* 73: 1–17.

Zhang, X., Liu, G. and Zheng, F. (2018). Understanding erosion processes using rare earth element tracers in a preformed interrill-rill system. *Sci. Total Environ.* 625: 920–927.

Zhao, Y., Yu, R., Hu, G., Lin, X. and Liu, X. (2017). Characteristics and environmental significance of rare earth elements in $PM_{2.5}$ of Nanchang, China. *J. Rare Earths* 35: 98–106.

Received for review, December 26, 2017
Revised, May 28, 2018
Accepted, June 11, 2018